Astron. Astrophys. 364, 479–490 (2000)

ASTRONOMY
AND
ASTROPHYSICS

Decoupled nuclei and nuclear polar rings in regular spiral galaxies

NGC 7217⋆

O.K. Sil'chenko[1,⋆⋆,⋆⋆⋆] **and V.L. Afanasiev**[2,†]

[1] Sternberg Astronomical Institute, University av. 13, Moscow 119899, Russia
[2] Special Astrophysical Observatory, Nizhnij Arkhyz, 357147 Russia

Received 21 July 2000 / Accepted 26 September 2000

Abstract. The regular isolated Sab galaxy NGC 7217 has been studied with the Multi-Pupil Fiber Spectrograph of the 6m telescope of the Special Astrophysical Observatory RAS (Nizhnij Arkhyz, Russia) in two spectral ranges, the blue one including the strong absorption lines Mg I and Fe I and the red one including the emission lines Hα and [N II]λ6583. We confirm the existence of a circumnuclear gaseous polar disk with a radius of 3″ which we reported earlier. The same area, with a radius of 3″–4″, elongated orthogonally to the line of nodes, is distinguished by high values of the Lick index $\langle$Fe$\rangle$ and shows a Mg/Fe ratio lower than solar. This implies that there were at least two discrete star formation bursts in the circumnuclear region with a temporal separation of a few Gyrs. We relate this pair of bursts to the complex structure of the global brightness profile of the galaxy, which may be decomposed into three exponential segments with different scalelengths.

Key words: galaxies: kinematics and dynamics – galaxies: structure – galaxies: spiral – galaxies: evolution – galaxies: nuclei – galaxies: photometry – galaxies: individual: NGC 7217

1. Introduction

A careful investigation of the inner parts in normal spiral galaxies with modern techniques reveals almost always a complicated structure which cannot be described by a classical two-component model consisting of a centrally concentrated, old, red, smooth de Vaucouleurs' bulge and a more extended, young, blue exponential disk with spiral arms. Among recent findings which may have serious implications for a global evolutionary picture we can mention papers on exponential bulges (Andredakis et al. 1995, Courteau et al. 1996), multi-tier disks – e.g. in NGC 5533 (Sil'chenko et al. 1997a) or in NGC 157 (Ryder et al. 1998), decoupled circumnuclear stellar disks (e.g. in NGC 4594, Emsellem et al. 1996), inner polar gaseous disks (e.g. in NGC 2841, Sil'chenko et al. 1997b), circumnuclear spiral arms (e.g. in NGC 5248, Laine et al. 1999, or in NGC 488, Sil'chenko 1999), etc. In some early-type spiral galaxies, e.g. in NGC 4138 (Jore et al. 1996) and in NGC 7217 (Merrifield & Kuijken 1994), the existence of counterrotating stars in their global disks was claimed. This may mean that discrete catastrophic events, such as minor mergers or gas accretion from a satellite, govern the evolution of even quite regular galaxies. But there may also exist some intrinsic evolutionary processes, such as bar formation and dissolution due to disk instabilities or mass concentration in the center, that can provide the same set of properties without any external action. We cannot yet prove either of these hypotheses because of the lack of detailed investigations of even nearby galaxies. So any new, careful analysis of the dynamics, structure, and stellar populations in normal spiral galaxies gives an additional chance to understand their evolution.

Here, we present a detailed study of the regular isolated Sab galaxy NGC 7217, the global parameters of which are given in Table 1. The galaxy has a prominent bulge and a truly flocculent spiral structure: unlike some other flocculent galaxies, e.g. NGC 2841 (Block et al. 1996) or NGC 5055 (Thornley & Mundy 1997) which unveil grand design in the NIR K-band, NGC 7217 preserves its non-wave appearance

Table 1. Global parameters of NGC 7217

Hubble type	(R)SA(r)ab
R_{25}	9.3 kpc
B_T^0	10.53
M_B	–20.5
$(B-V)_T^0$	0.77
$(U-B)_T^0$	0.25
V_r	952 $km \cdot s^{-1}$
Distance	16.4 Mpc (H_0=75 $km \cdot s^{-1} \cdot Mpc^{-1}$)
$i(phot)$	35^o
$PA(phot)$	95^o

Send offprint requests to: O.K. Sil'chenko (olga@sai.msu.su)

⋆ Partly based on observations collected with the 6m telescope of the Special Astrophysical Observatory (SAO) of the Russian Academy of Sciences (RAS) which is operated under the financial support of Science Department of Russia (registration number 01-43) and on data from the ING Archive and the HST Archive.

⋆⋆ Isaac Newton Institute of Chile, Moscow Branch
⋆⋆⋆ UK Astronomy Data Centre, Guest Investigator
† Isaac Newton Institute of Chile, SAO Branch

Table 2. Spectral observations of NGC 7217

Date	Telescope	Configuration	Exposure	Scale	Spectral range	Dispersion	PA(top)
19.08.98	6m BTA	MPFS+CCD 1024×1024	60 min	$1''.0$ per lens	4250–5600 Å	1.3 Å/px	215°
19.08.98	6m BTA	MPFS+CCD 1024×1024	60 min	$1''.0$ per lens	5650–7000 Å	1.3 Å/px	215°
06.01.91	4.2m WHT	ISIS+CCD 800×1180	25 min	$0''.335$ per px	8000–8840 Å	0.74 Å/px	240°
07.01.91	4.2m WHT	ISIS+CCD 800×1180	20 min	$0''.335$ per px	5830–6680 Å	0.74 Å/px	150°
07.01.91	4.2m WHT	ISIS+CCD 800×1180	20 min	$0''.335$ per px	5830–6680 Å	0.74 Å/px	240°
06.11.97	4.2m WHT	ISIS+CCD 1024×1024	33 min	$0''.335$ per px	6150–7000 Å	0.8 Å/px	68°

even at $2\,\mu m$ (Elmegreen et al. 1999). But it has another puzzling morphological feature, namely, three stellar rings at radii of $12''$, $32''$, and $77''$, the innermost of which is accompanied by Hα emission enhancement and the outermost also by HI concentration, so both are sites of intense star formation (Buta et al. 1995). Such star forming rings are usually treated as resonance loci of a bar. But morphologically NGC 7217 is a purely unbarred galaxy; besides, a bar should produce a wave spiral pattern which is not observed in this galaxy. Buta et al. (1995) tried to solve this problem, through a Fourier analysis of the I-band image of NGC 7217, and found a mode m=2; the conclusion was that the galaxy has a low-contrast bar aligned along $PA \approx 60^\circ$. Perhaps, this bar is observed in the late stage of dissolution: as Athanassoula (1996) has discussed, the rings are more long-lived than the bars, which may be destroyed by a central mass concentration. But the most striking peculiarity has been found by Merrifield & Kuijken (1994): they have claimed the existence of a counterrotating stellar disk. More exactly, from the analysis of stellar line-of-sight velocity distribution (LOSVD) data they noted a counterrotating "wing" over the full radius range, which they have studied, namely from $R = 10''$ to $R = 60''$. This "wing" contains 30% of all stars and does not become weaker with radius; so they conclude that it is not a bulge, but a counterrotating fraction of the global disk. Immediately, the question has been raised about secondary gas infall or a minor merger, though the galaxy looks quite isolated.

We have already studied this interesting galaxy (Zasov & Sil'chenko 1997): from the ionized gas kinematics in the circumnuclear region and from an analysis of the central isophotes we have detected an inclined gaseous disk in the very center of NGC 7217 and reported a mass concentration of $6 \cdot 10^7\,M_\odot$ in its nucleus. During the last years our understanding was growing on how the phenomena of chemically distinct galactic cores (Sil'chenko et al. 1992) and kinematically decoupled gaseous or stellar subsystems in disk galaxies may be related, both being produced by a secondary gas accretion or minor merger event. For example, in NGC 2841 we have found a chemically distinct nucleus, a circumnuclear polar disk of ionized gas with a radius of 200 pc, and counterrotating stars in the bulge (Sil'chenko et al. 1997b, Afanasiev & Sil'chenko 1999). The similarity between the gas and stellar kinematics in NGC 2841 and NGC 7217 has stimulated us to search for a chemically distinct nucleus in the latter galaxy. The results of this search, together with additional kinematical and photometric analyses, are presented in this paper.

2. Observations and data reduction

In 1998 we have undertaken two-dimensional spectroscopy of NGC 7217 with the Multi-Pupil Fiber Spectrograph (MPFS) of the 6m telescope of the Special Astrophysical Observatory (Nizhnij Arkhyz, Russia). Two spectral ranges were exposed: a blue-green one, 4250–5600 Å, and a red one, 5650–7000 Å. The detailed parameters of the spectral observations are given in Table 2. A grating of 1200 grooves per mm was used which provided a reciprocal dispersion of 1.3 Å per pixel and a spectral resolution of 3 Å. The seeing of FWHM=$1''.6$ was estimated from a stellar exposure.

These spectral observations have been made with the new variant of the panoramic spectrophotometer which became operational at the prime focus of the 6m telescope in the end of 1997. With respect to the previous variants of MPFS (Afanasiev et al. 1990, Afanasiev et al. 1996), the field of view is now increased and the common spectral range is larger due to the use of fibers: they transmit light from 16×16 square elements of the galaxy image to the slit of the spectrograph (256 fibers) together with the sky background taken $4'.5$ away from the galaxy itself (6 fibers). The size of one spatial element is $1'' \times 1''$. At the exit of the spectrograph a 1024×1024 CCD registers all 262 spectra simultaneously. The primary reduction of the data is made within IDL. After bias subtracting, flatfielding, and one-dimensional spectra extraction from the CCD frame, we linearize and analyse each spectrum individually. The one-element spectral characteristics, such as fluxes in continuum or in emission lines, redshift, and absorption-line indices are then combined into two-dimensional arrays corresponding to the galactic region under consideration with the help of software developed earlier in the Special Astrophysical Observatory (Vlasyuk 1993) and with our own programs. To calculate absorption-line indices and their errors we have used also the program of Dr. Vazdekis. As a result, we obtain two-dimensional surface brightness distributions, velocity fields, and maps of stellar population characteristics. In the blue-green spectral range, we measure the absorption-line indices Hβ, Mgb, Mg_2, Fe5270, and Fe5335 in the popular Lick system (Worthey et al. 1994); to check the consistency of our measurements with the model indices calculated in this system (Worthey 1994), we also observed stars from their list (Worthey et al. 1994). Besides that, we use our blue-green spectra to derive a stellar velocity field in the center of NGC 7217 by cross-correlating elementary galactic spectra with the spectrum of a K-giant star – the brighter component of the visual

binary STF 2788. In the red spectral range we have measured baricentric positions of the emission line [N II]λ6583, which is the strongest in the center of NGC 7217, to derive a velocity field of the ionized gas. We have estimated the best accuracy of our velocity measurements as 10 km s^{-1} from the night-sky line [OI]λ6300 analysis. For the absorption-line index accuracy, we have made estimates using the method of Cardiel et al. (1998): the typical error of the indices varies for the EW-like indices from 0.15 Å in the nucleus to 0.5 Å in the individual elements at the edges of the area investigated, and from 0.004 to 0.01 for Mg_2. To keep a constant level of accuracy along the radius, we summed the spectra in concentric rings centered on the nucleus and studied the radial dependencies of the absorption-line indices by comparing them to the synthetic models of old stellar populations of Worthey (1994) and Tantalo et al. (1998). We estimate the mean accuracy of our azimuthally-averaged indices as 0.1 Å.

Also, we have taken several long-slit spectra of NGC 7217, which have been obtained at the William Herschel Telescope on La Palma with the ISIS, from the ING Archive. The details of exposures are also given in Table 2. These CCD frames have been reduced with the software of Dr. Valeri Vlasyuk (Vlasyuk 1993).

The photometric data involved in our analysis are taken from the ING and HST Archives. The broad-band I image of NGC 7217 has been obtained on June 1st, 1998, at the 1m Jacobus Kapteyn Telescope on La Palma. The exposure times were 10 min, 10 min, and 5 min, but only the first of the exposures was well guided; only this is analysed in this work. The seeing quality is estimated from neighbouring star measurements as $FWHM_* = 1\farcs5$. The central part of the galaxy has been also observed by the Hubble Space Telescope. The earlier observations with WFPC2 were made on June 10, 1994, through the filter F547M, with an exposure time of 5 min (Principal Investigator: W. Sargent, Program ID: 5419). Later, it was observed with the NICMOS2 through the filters F110W and F160W during 128 sec each on August 17, 1997 (Principal Investigator: M. Stiavelli, Program ID: 7331). The spatial resolution was $0\farcs1$ for WFPC2 observations and $0\farcs2$ for the NICMOS observations. We have derived morphological characteristics of the surface brightness distribution in NGC 7217 by analysing these images. The program FITELL of Dr. Vlasyuk has been used for tracing the isophote major axis position angle and ellipticity along the radius, and 2D image decomposition was performed with the software FVIZ and IMAR (Vlasyuk 1993) as well as with our own programs.

3. A magnesium distinct nucleus and a Fe-rich circumnuclear disk

To study properties of the stellar populations in the central regions of galaxies, we use metal- and hydrogen-line indices confined to a rather narrow green spectral range, namely, Hβ, Mgb, Fe5270, and Fe5335. In the case of NGC 7217 there are some problems with these indices, however. First of all, rather intense Hα emission is observed in the center of the galaxy, except in the narrow radial range of $R = 4'' - 6''$. Therefore one can expect that the absorption-line index Hβ, which is a good indicator of stellar population age, will be strongly contaminated by the emission almost everywhere and therefore cannot be used. Secondly, in the nucleus itself a noticeable emission line [N I]λ5200 is seen, and as Goudfrooij & Emsellem (1996) noted, this emission causes an overestimation of the absorption-line index Mgb because it falls into the continuum band of this index. Therefore we are forced to use an index Mg_2 which has a broader continuum base than Mgb, but is more dependent on the correct calibration of the global spectrum shape. To calculate Mg_2, we use galactic spectra calibrated into absolute fluxes.

Fig. 1 shows the isocontours of two-dimensional distributions of the Lick absorption-line indices, Mg_2 (left) and $\langle$Fe$\rangle \equiv$ (Fe5270+Fe5335)/2 (right) in the central $16''$ of NGC 7217. The magnesium index is strongly peaked near the nucleus; it decreases rather symmetrically with radius, and the shape of outer Mg_2 contours is not too different from the shape of continuum isophotes. However, in the very center an elongated structure seems to appear at the limit of the spatial resolution; it is a bit shifted to the east from the center of the brightness distribution. The distribution of the iron index is much more complicated. In the patchy pattern, one can distinguish an elongated structure of enhanced $\langle$Fe$\rangle \equiv$ (Fe5270+Fe5335)/2, also shifted to the east from the nucleus and much more extended than the analogous structure in the Mg_2 map: it can be traced up to $R \approx 5''$. We shall refer to it as the 'Fe-rich disk'; in the next sections we will argue that it can be indeed related to the circumnuclear stellar disk. However, let us note here that the structure with the enhanced metal absorption lines is elongated in the south-north direction whereas the global line of nodes is oriented approximately east-west (see Table 1).

Lick absorption-line indices have been well calibrated with respect to the integrated (luminosity-averaged) properties of stellar populations in numerous works using evolutionary synthesis techniques. Our conclusions derived below are based on the models of Worthey (1994) and Tantalo et al. (1998) for single-age single-metallicity stellar populations. Diagnostic diagrams of index vs. index are presented in Fig. 2. The diagram $\langle$Fe$\rangle$ vs. Mg_2 (left) is being considered by many specialists in chemical evolution as a tool to limit the duration of the main star formation episode (see, e.g., Matteucci 1994). When Worthey et al. (1992) noted for the first time a magnesium overabundance in most bright elliptical galaxies, this phenomenon was soon treated as a natural consequence of the short duration of their star forming epoch, less than 1 Gyr. The nature of this effect is deduced from the theoretical prediction that magnesium has to be produced mainly by SNeII, which explode earlier than the bulk of the iron-producing SNeIa from the same stellar generation; if the star formation process stops between these two moments, the stars would have a higher magnesium-to-iron ratio than the solar, which corresponds to continuous star formation. The star formation histories in the centers of early-type disk galaxies are less clear than those in ellipticals, and observational results on their Mg/Fe ratios are also contradictory. Our statistics (Sil'chenko 1993) showed evidence for a solar Mg/Fe ratio in the centers of almost all disk galaxies, from Sc

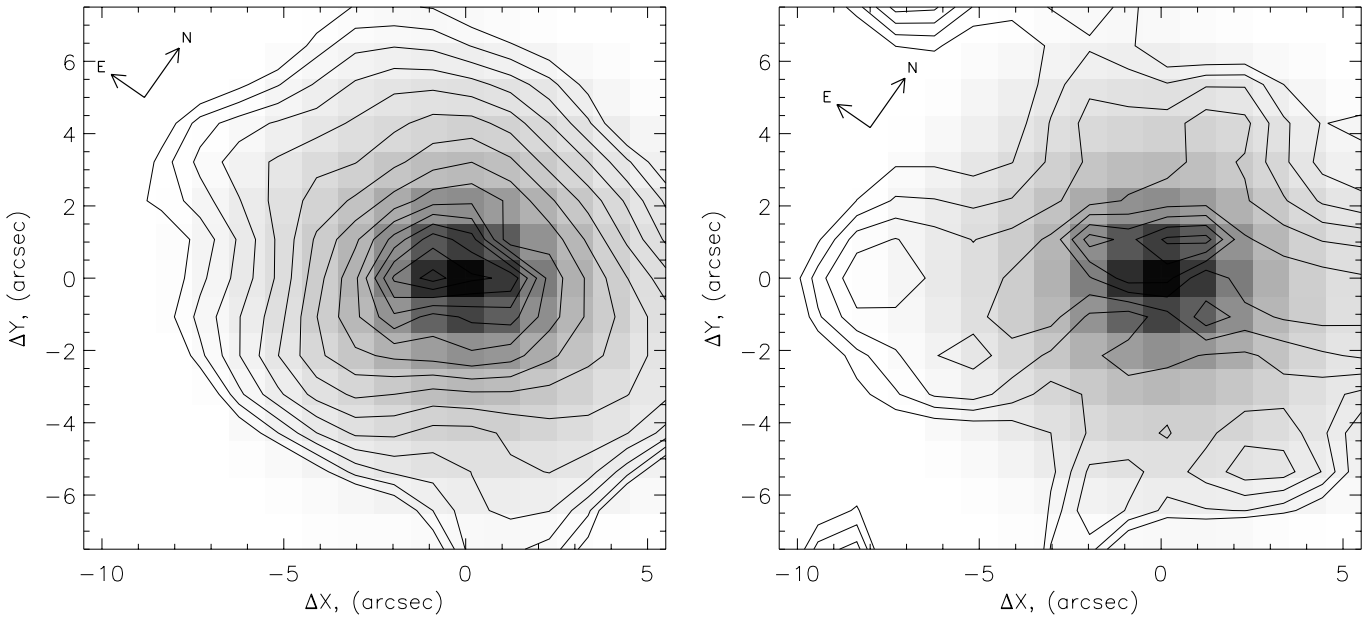

Fig. 1. Two-dimensional maps of the Lick absorption-line indices (isocontours) in the central region of NGC 7217: Mg_2 (left, the outermost isocontour corresponds to 0.180, the step between isocontours is 0.005) and ⟨Fe⟩ (right, the outermost isocontour corresponds to 2.50 Å, the step between isocontours is 0.1 Å). The gray-scaled background is the distribution of the green continuum.

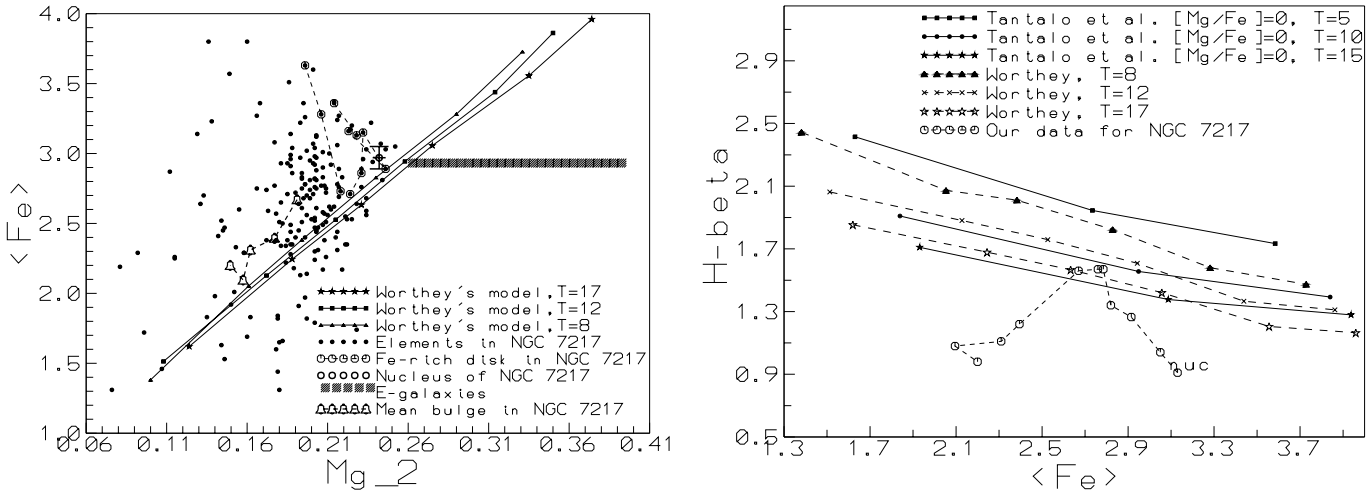

Fig. 2. Comparison of our observational data for NGC 7217 with the models of Worthey (1994) and Tantalo et al. (1998) for [Mg/Fe]=0. The ages of the models in the legend are given in billion years. The observational points connected by a dashed line – bells in the diagram ⟨Fe⟩ vs Mg_2 (left panel) and circles in the diagram Hβ vs ⟨Fe⟩ (right panel) – are azimuthally averages and taken along the radius with a step of $1\farcs0$, the bulge points starting from $R = 6''$; the points for the Fe-rich disk in the left panel are connected from its northern end to the southern one; unconnected observational points are for individual elements. The metallicities for Worthey's models are +0.50, +0.25, 0.00, –0.22, –0.50, –1.00, if one takes the signs along the sequences from the right to the left, and for the models of Tantalo et al. they are +0.4, 0.0, and -0.7. The mean data for ellipticals of intermediate luminosity on the left panel are taken from Trager et al. (1998).

to S0, in both bulge- and disk-dominated objects. Jablonka et al. (1996) reported a strong magnesium overabundance, up to [Mg/Fe]$\geq +0.5$, in bulges brighter than $M_r \approx -19.5$, including our target galaxy NGC 7217. Our data in Fig. 2 (left) differs from those of Jablonka et al.: here, the nucleus of NGC 7217 lies near the model sequences of Worthey (1994) implying a solar Mg/Fe ratio or even a slight iron overabundance. This result is due to a smaller Mg_2 estimate, 0.25 instead of 0.28 in Jablonka et al. (1996), but mainly to a higher Fe5335 value, 3.0 Å instead of 2.4 Å. Curiously, the estimate of Fe5270 made by Jablonka et al. (1996) is quite consistent with ours. We cannot explain the cause of the agreement in Fe5270 and the disagreement in Fe5335 but we would like to note that in model calculations (e.g. see Worthey 1994) the values of Fe5270 and Fe5335 obtained are almost equal to each other, as is the case in our data.

The points related to the bulge of NGC 7217 are dispersed around the model sequences with a solar magnesium–to–iron ratio, and none of them fall into the area occupied by ellipticals of similar luminosity ($M_B = -19 \div -20$), whose mean locus is plotted using the data from Trager et al. (1998) (a shaded horizontal band in Fig. 2, left). The azimuthally-averaged measurements for the bulge also lie along the sequences for [Mg/Fe]=0. But the most interesting behaviour is demonstrated by the points taken within the Fe-rich circumnuclear disk. In this rather bright, central part of the galaxy, the accuracy of the arcsecond element indices, of, say, $\langle$Fe$\rangle$, is better than 0.3 Å. The deviations of the extreme points of the Fe-rich disk at $R \approx 5''$ from the model sequence [Mg/Fe]=0 are at the 3σ level, and certainly due to iron overabundance. This is a rather puzzling observational phenomenon common for some types of irregular galaxies (e.g. the LMC), and it is usually treated as evidence for a bursty character of the star formation (Gilmore & Wyse 1991, Marconi et al. 1994). When approaching the center of the disk, the Mg/Fe ratio rises and near the nucleus it becomes close to solar. The total metallicity of the circumnuclear disk is higher than that of the bulge. Obviously, the Fe-rich disk is a secondary formation product. The star formation within it had to be strongly inhomogeneous, with an exotic mechanism to result in iron overabundance at its outer edge: a kind of transient star forming circumnuclear ring.

As we mentioned earlier, the age diagnostics in the center of NGC 7217 is complicated by the noticeable Balmer emission contaminating the Lick index Hβ. So in the diagram Hβ vs. $\langle$Fe$\rangle$ (Fig. 2, right) the majority of the observational points trace only upper limits for the age of the stellar population. But in the narrow gap between the LINER nucleus and the star forming ring (see Sect. 5), at $R = 4'' - 6''$ the Hα emission is absent and we can use the Hβ absorption-line index to estimate a luminosity-weighted age of the bulge stellar population. From Fig. 2 (right) one can see that the bulge of NGC 7217 is rather old, at least 10 Gyr. The ages of the nucleus and of the Fe-rich circumnuclear stellar disk cannot be determined exactly.

4. Kinematics of stars and gas in NGC 7217

4.1. Circumnuclear region

In the previous paper (Zasov & Sil'chenko 1997) we noted clear signatures of the dynamical distinctness of the nucleus in NGC 7217: the rotation axis of the ionized gas inside $R \approx 5''$ turns by almost 90°. Now we present further proofs of the existence of a circumnuclear 'polar' gaseous ring (disk?) in this galaxy.

We now proceed to determine the parameters of the stellar and gaseous rotation around the nucleus of NGC 7217. Under the assumption of planar axisymmetric rotation, the azimuthal dependence of central line-of-sight velocity gradients is:

$$dv_r/dr = \omega \sin i \cos(PA - PA_0),$$

where ω is the deprojected central angular rotation velocity, i is the inclination of the rotation plane and PA_0 is the orientation of the line of nodes, coinciding in the case of an axisymmetric ellipsoid (or a thin disk) with the photometric major axis. So by fitting azimuthal variations of the central line-of-sight velocity gradients with a cosine curve, we can determine the orientation of the dynamical major axis by its phase and the central angular rotation velocity by its amplitude. To apply this procedure, we need two-dimensional velocity fields.

The new MPFS observations allow us to construct two-dimensional velocity maps for the central $16'' \times 16''$ region of NGC 7217. Fig. 3 shows such maps for the stars (left) and for the ionized gas as traced by the [N II]λ6583 emission (middle), as well as the stellar velocity dispersion map (right). One can see that two velocity maps look different. At first glance, the dynamical major axis of the stellar component seems to be close to the global line of nodes, west-east. However it is strange that the brightness center coincides with a flat area in the velocity map. If the dynamical center coincides with the brightness center, we would obtain a central projected angular rotation velocity of only (8 ± 2) km/s/arcsec. If we shift the dynamical center $3''$ to the east, to the point of maximum isovelocity crowding, we can increase $\omega_{proj} \equiv \omega \sin(i)$ to (22 ± 5) km/s/arcsec. Fortunately, the direction of the maximum line-of-sight velocity gradient, or the dynamical major axis, remains the same for both dynamical center locations: it is $PA_{dyn} = 241° \pm 2°$ within $R = 3''$, some 30° different from the line-of-nodes direction, but coinciding with the PA of the low-contrast bar reported by Buta et al. (1995). Outside $R \approx 3''$ the dynamical major axis turns to $PA_{dyn} = 276°$, implying an axisymmetric stellar rotation parallel to the symmetry plane of the galaxy. The velocity map for the ionized gas obtained by measuring the baricenters of the [N II] emission line (Hα is less relevant because of the underlying absorption line) looks even more striking than that for the stars. The isovelocities in the very center demonstrate a strong so-called "S-shape" distortion, whose dynamical major axis direction changes by 90° in the radius range of $3''$–$7''$. By fitting a cosine curve to the line-of-sight velocity gradients within $3''$ from the center, we obtain a projected angular rotation velocity of (17 ± 7) km/s/arcsec and a dynamical major axis $PA_{dyn} = -31° \pm 4°$, orthogonal to the dynamical major axis of the stars in this radius range. Again, we find the signature of a circumnuclear polar gaseous disk.

The two-dimensional map of the stellar velocity dispersion in the central $16''$ region (Fig. 3, right) looks somewhat peculiar: though rather smooth, it demonstrates an elongated 'saddle' of relatively low σ_*, at about $\sigma_* \approx 130\,\mathrm{km\,s^{-1}}$, in $PA \approx 60°$ and a slight increase of σ_* along the kinematic minor axis on both sides of the nucleus. We have never seen anything like this and cannot give an interpretation of this map. The dynamical center which we define here as a center of symmetry of the stellar velocity dispersion map again seems to be shifted to the east of the brightness center.

We can check our result on the decoupled rotation of the circumnuclear ionized gas with the long-slit spectral data from the ING Archive. Fig. 4 shows line-of-sight velocities measured from [N II]λ6583 and Hα emission lines in $PA = 68°$ and $PA = 150°$. In $PA = 68°$, not too far from the line of nodes,

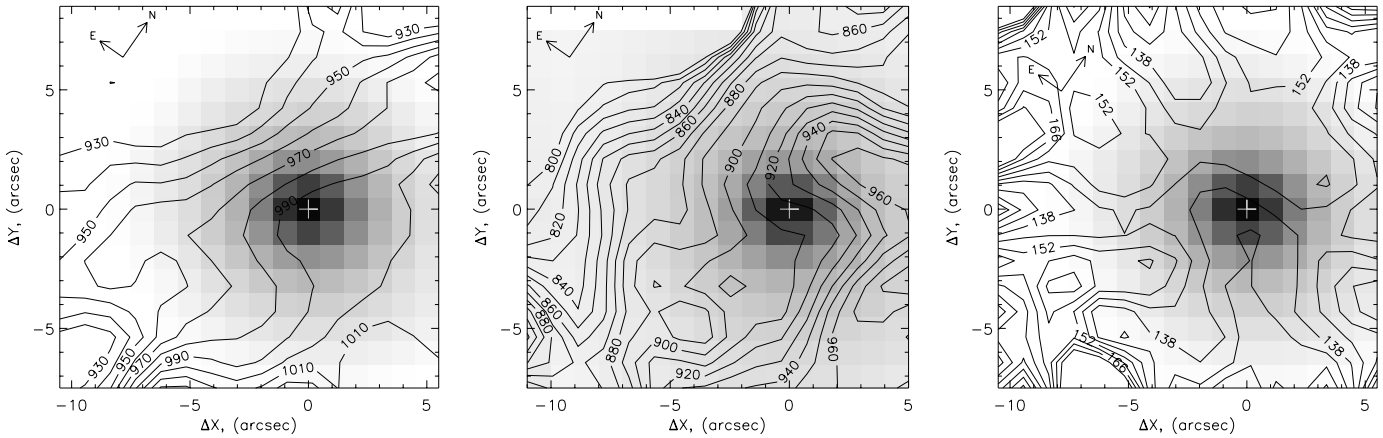

Fig. 3. Two-dimensional line-of-sight velocity fields for the stars (left) and for the ionized gas (middle), and the map of the stellar velocity dispersion (right) in the central $16'' \times 16''$ of NGC 7217. The gray-scaled background represents the continuum distribution in the green for the stars and in the red for the gas.

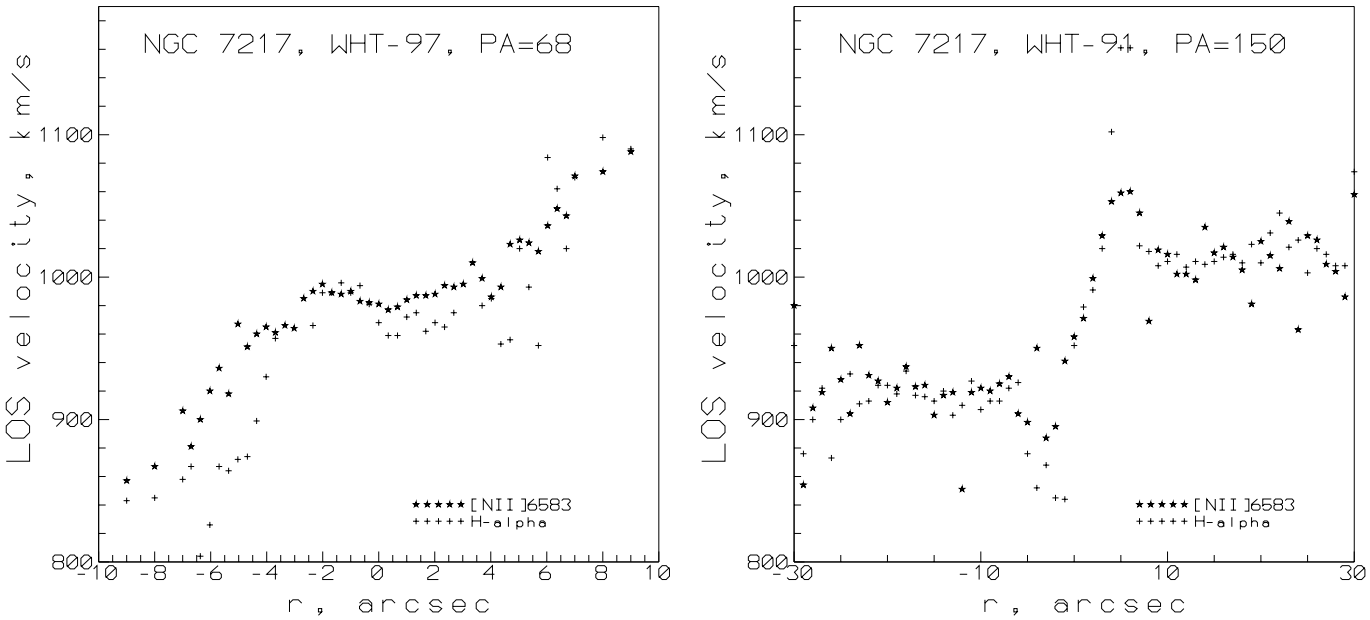

Fig. 4. Long-slit position-velocity cross-sections in $PA = 68°$, not too far from the line of nodes, (left) and $PA = 150°$ (right) for the center of NGC 7217; [N II] and Hα emission line measurements are plotted.

one can see a flat velocity profile segment in the very center, till $\pm 3''$ from the nucleus, implying that the dynamical major axis of the circumnuclear ionized gas is aligned orthogonally, in $PA \approx 158°$ (or –22°). Outside this central region the gas shows much larger projected velocities with respect to the nucleus. In $PA = 150°$, consistent with the previous cross-section, the central part of the velocity profile shows fast decoupled rotation within $\pm 4''$ from the nucleus with a slope of 24 km/s/arcsec – evidently, this direction is close to the dynamical major axis of the circumnuclear gas; outside the radius of $4''$ the projected rotation velocity falls to a half of the maximum value reached at the $4''$ radius. Therefore, the long-slit cross-sections confirm the dynamical distinctness of the central region of NGC 7217 within a radius of $3''$–$4''$ and the existence of a 'polar' circumnuclear gaseous disk rotating in a plane orthogonal to the global plane of the galaxy.

4.2. The whole galaxy

Kinematics of the ionized gas in NGC 7217 has been studied more than once. Long-slit cross-sections along the major axis were obtained by Peterson et al. (1978), Rubin et al. (1985), and Buta et al. (1995), and our team also observed NGC 7217 with a long-slit spectrograph and a scanning Fabry-Perot interferometer at the 6m telescope (Zasov & Sil'chenko 1997). We have now analyzed the Hα and [N II]λ6583 emission lines in the three additional long-slit cross-sections taken from the ING Archive. The results obtained over the full radius range are quite

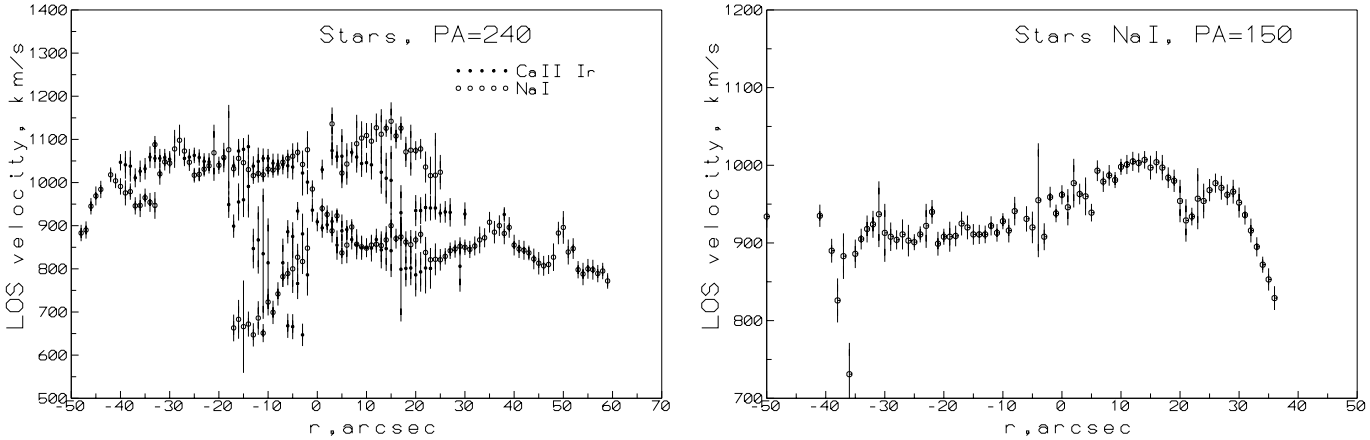

Fig. 5. Long-slit cross-sections in $PA = 240^\circ$ (left) and $PA = 150^\circ$ (right) of NGC 7217; stellar absorption line measurements obtained by cross-correlation with the template star spectrum are plotted.

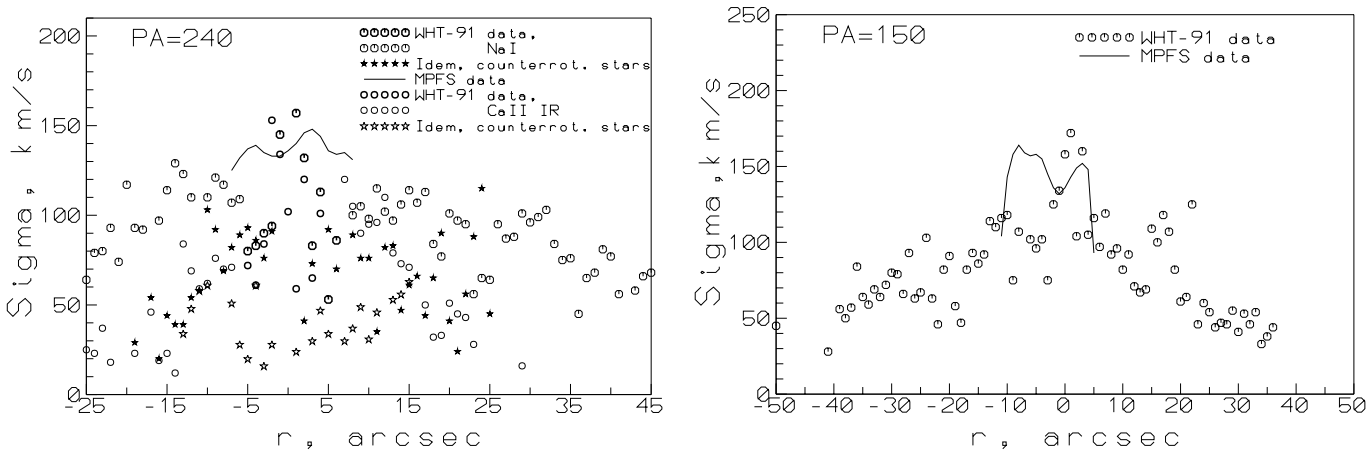

Fig. 6. Long-slit cross-sections in $PA = 240^\circ$ (left) and $PA = 150^\circ$ (right) of NGC 7217; stellar velocity dispersions obtained by cross-correlation with the template star spectrum are plotted. Also the cuts simulated with the MPFS data in the corresponing position angles are given.

consistent with the velocity curves published previously, and we do not present the raw velocity data here.

The stellar kinematics in NGC 7217 have received much less attention than the gas kinematics. Merrifield & Kuijken (1994) cross-correlated absorption spectra taken along the major and minor axes in the spectral range near Mgbλ5175 with those of template stars, and reported a clear evidence of the presence of a counterrotating stellar subsystem in the disk of NGC 7217: LOSVDs of stars look double-peaked in the full radius range considered by Merrifield & Kuijken (1994), i.e., up to $60''$ from the center. However, their work lacks direct measurements of the velocities of the co-rotating and counter-rotating components, after their separation in the spectra, as well as estimates of velocity dispersions, so their conclusion that the counter-rotating component is a part of the global disk of the galaxy is not very convincing, as it is only based on an ambiguous photometric decomposition. We have calculated stellar velocity profiles for two spectra in $PA = 240^\circ$, one near the Na Iλ5890,5896 lines and another near the Ca II Ir triplet, and for one spectrum near Na I in $PA = 150^\circ$ through an interactive Gauss analysis of the cross-correlation peaks (as a template star, we have taken HR 661). The results are presented in Figs. 5 and 6. We confirm the existence of the counter-rotating stellar component seen in the cross-sections not far from the major axis, in $PA = 240^\circ$. But its velocity profile (Fig. 5, left) does not represent a simple mirror picture of the main co-rotating component. While the main rotation curve is rather flat between $R \approx 10''$ and $30''$, the counter-rotating component has a peak near $R = 10'' - 15''$ and then already falls back to the systemic velocity at $R \approx 20''$. If the result obtained by Merrifield & Kuijken (1994) for major-axis cross-section differing by 30° in PA from ours is true, i.e., if two maxima of LOSVD are located symmetrically with respect to the systemic velocity, this may signify that the planes of rotation of the co-rotating and counter-rotating stars are different. The counter-rotating stellar subsystem may rotate faster than the co-rotating one; the reason for this can be found in Fig. 6. The stellar velocity dispersion in NGC 7217 is strongly peaked near the nucleus where it reaches about 160 km s^{-1} (previous estimates: 185 ± 18 km s^{-1}, Whitemore et al. 1979; 122 ± 3 km s^{-1}, Dressler 1984). In both

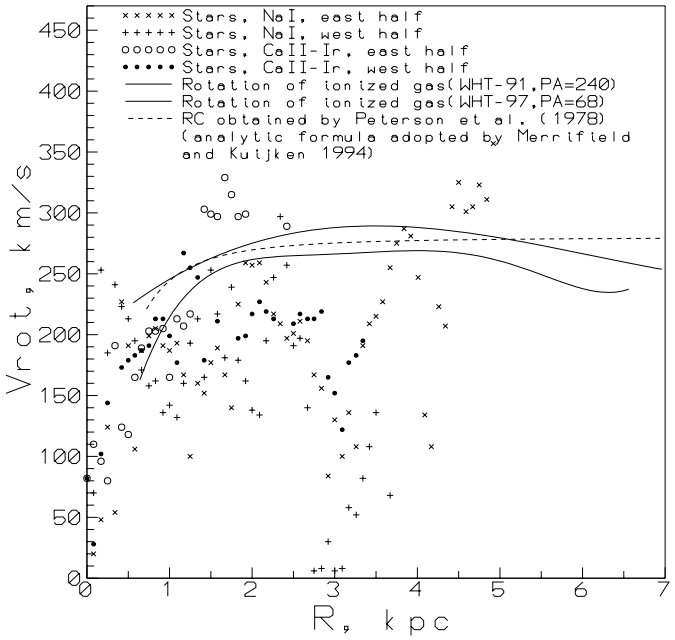

Fig. 7. Deprojected rotation curves for the ionized gas (lines) and for the stars (signes) in NGC 7217. The east and west halves of the galaxy are shown by different signes

directions, in $PA = 240°$ and $PA = 150°$, it falls rapidly with radius and becomes less than 100 km s^{-1} at $R \geq 5''$. But the velocity dispersion of the counter-rotating component seems to be systematically lower than that of the co-rotating one, so since both rotate in the same potential, the former has the faster rotation. As the stellar velocity dispersion of the counter-rotating component is of order of 50 km s^{-1}, we can surely state that it is in a disk, so the guess of Merrifield & Kuijken (1994) has been correct.

In Fig. 7 we compare the stellar and gaseous rotation curves deprojected with the orientation parameters $PA_0 = 85°$ and $i = 35°$ from the data noted in the legend. All three gas rotation curves, the one from Peterson et al. (1978) as approximated by the analytic formula in the paper of Merrifield and Kuijken (1994) and our two, from the WHT-91 cross-section in $PA = 240°$ and from the WHT-97 cross-section in $PA = 68°$, are in general agreement with each other: they are flat, with a maximum velocity level of $v_{rot} \approx 270$ km s^{-1} and a possible decrease by some 20 km s^{-1} in the radius range of 4.5–6 kpc. The stellar rotation looks more irregular though we have taken into consideration the main component only, i.e. the brighter which is co-rotating with the gas. The highest values of stellar rotation velocities are comparable to the gas ones, thus supporting the idea of disk predominance at already $R \approx 1$ kpc – in favour of Kent's (1986) photometric decomposition (see the next section). But in many places the stellar rotation velocities fall below the gas rotation curve. The most striking feature of this kind is seen around $R = 3$ kpc: at different directions and wavelengths (implying: for stars of different ages?) the stellar velocity is 50% –100% less. Interestingly, a similar detail at the same radius was found by us in the azimuthally averaged rotation curve obtained for the ionized gas with the scanning Fabry-Perot interferometer (Zasov & Sil'chenko 1997). We noted that this feature is located at the outer edge of the inner pseudoring and perhaps related to some non-circular motions; but no detailed interpretation was given. Now, when we detect an even stronger response to the ring in a dissipationless dynamical subsystem, we are even more astonished about the nature of the inner pseudoring.

5. Surface photometry and central structure of NGC 7217

5.1. The central region of NGC 7217

From our red exposure with the MPFS we have derived the surface distributions of the emission-line intensities of Hα and [N II]λ6583, as well as of their ratio (see Fig. 8). NGC 7217 is a LINER, so the nitrogen emission is the strongest in its center; its distribution (Fig. 8, top) is concentrated towards the center, but still well resolved. The inner isophotes of the nitrogen emission seem to be elongated approximately north-south, i.e. orthogonally to the global line of nodes, but close to the dynamical major axis orientation found in the previous section for the circumnuclear ionized gas. The surface distribution of the Hα emission (Fig. 8, middle) differs from that of [N II]λ6583: it demonstrates an emission ring with the radius of $11''$, as previously found by Pogge (1989). Besides the ring, a central concentration also aligned along the north-south direction is present. The [N II]–to–Hα ratio (Fig. 8, bottom) varies significantly over a tiny area with a radius of $11''$: it is 0.5 in the Hα-ring, slightly above 1 at the inner edge of the Hα-ring, 4 in the nucleus and 5–10 at the edge of the central emission concentration. We can easily understand the [N II]–to–Hα ratios in the ring and in the nucleus, as they are typical for a star formation site and for LINER excitation, respectively, but the high [N II]–to–Hα ratio at the inner edge of the ring and at the outer edge of the central concentration needs further explanation. Buta et al. (1995) considered the rings in NGC 7217 in detail and noted that the Hα-ring coincides with the continuum (B-band) ring, but inside of both there is a dust ring. Similar shifts between the stellar (gaseous) and dust features are observed in spiral arms and large-scale bars, and there they are attributed to shocks. Our high [N II]–to–Hα ratios in the center of NGC 7217 could be explained if the circumnuclear gaseous ring has a radial velocity component toward the center and if the central ionized gas disk is inclined with respect to the plane populated by surrounding gas: then shocks would be arisen in the required locations.

In our previous work (Zasov & Sil'chenko 1997) we reported a turn of the isophote major axis and an increase of ellipticity inside $R = 1''$ using HST WFPC2 data obtained through the F547M filter (the pivot wavelength is 5487 Å). But dust, which is obviously present in the center of NGC 7217, might distort the true shape of the brightness (mass) distribution. Now we add NICMOS data at 1.1 μm and 1.6 μm which are much less affected by dust. A comparison of the NICMOS and WFPC2 data (Fig. 9) shows their consistensy: indeed, the isophote major axis turns by $\approx 90°$ and the ellipticity increases in the very center of the galaxy. The central gravitational potential shape in

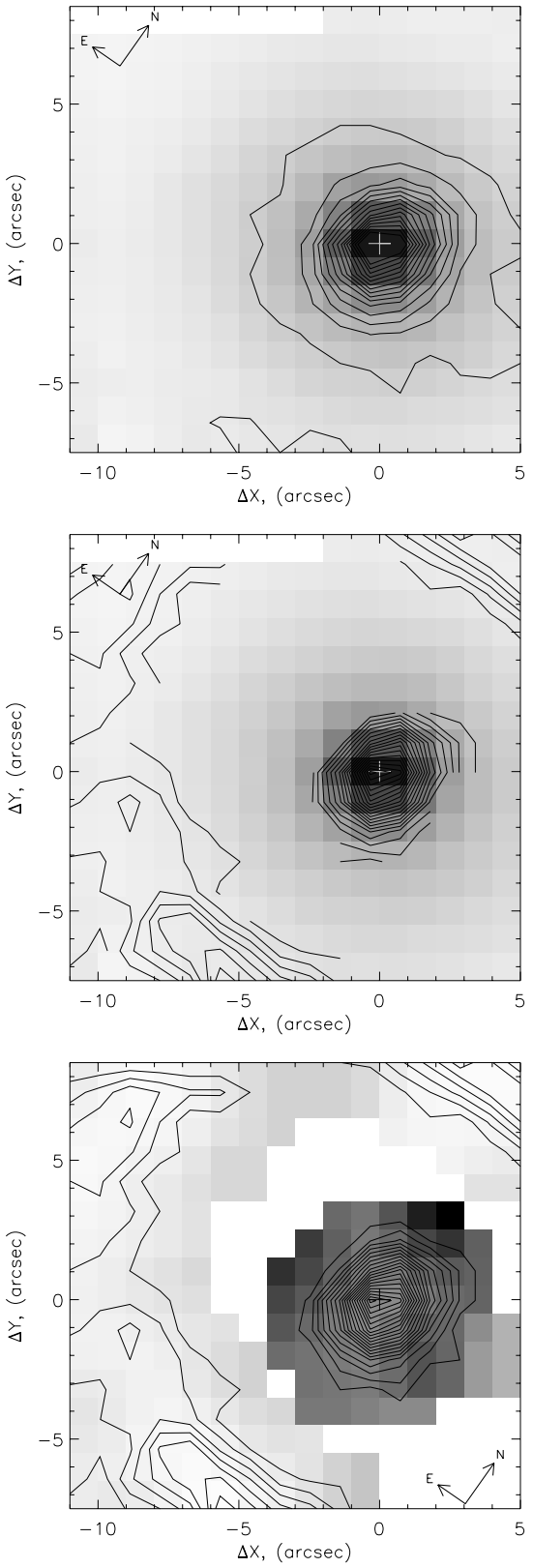

Fig. 8. Isocontours of two-dimensional maps of the surface brightness distributions for the emission lines [N II]λ6583 (top) and Hα (middle) in the center of NGC 7217: the gray-scaled background is the red continuum distribution, in arbitrary units; the bottom panel presents their intensity ratio (gray-scaled) overlaid by Hα isophotes.

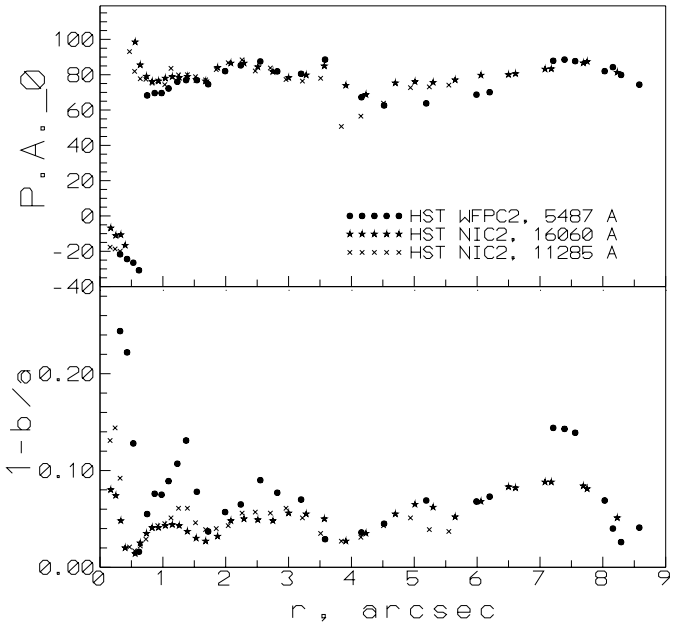

Fig. 9. Radial variations of the isophote morphological characteristics in NGC 7217 according to the data obtained with the WFPC2 and NICMOS of the Hubble Space Telescope.

NGC 7217 may be an ellipsoid with a polar orientation of the projected largest axis, or an axisymmetric ellipsoid with the line of nodes orthogonal to the global plane of the galaxy. The latter suggestion is consistent with the alignment of the dynamical major axis of the circumnuclear ionized gas: this coincidence proves the circular rotation of the gas in the polar plane. The radius of the polar gaseous disk, some 3″ (250 pc), is larger than the visible extent of the polar orientation of the photometric major axis, but as we see in the end of this section, the polar stellar structure is more extended than it can be deduced from the analysis of the integrated surface brightness alone – a decomposition of global structural components is necessary. We would only note that the orientation of the dynamical major axis of the stars within 3″ from the nucleus implies a prolate form of the central stellar structure.

5.2. The whole galaxy

Photometric analysis of the global structure of NGC 7217 has a long history. Boroson (1981) tried to decompose the major axis brightness profile in the B-band, but unsuccessfully, because multiple blue rings made the B-band profile very irregular. Kent (1986) analysed a 2D image in the r-band, more regular than that in B, and decomposed it into a de Vaucouleurs' bulge and an exponential disk, with a 1:3 luminosity ratio. According to this decomposition, the exponential disk becomes the dominant component at $R \geq 20''$. However, there are other, quite different variants of decomposition. Buta et al. (1995) obtained a de Vaucouleurs' bulge which dominates over the full radius range, with a total bulge-to-disk luminosity ratio of 2.3–2.4. A similar result was obtained by Baggett et al. (1998). Our analysis of the bright-

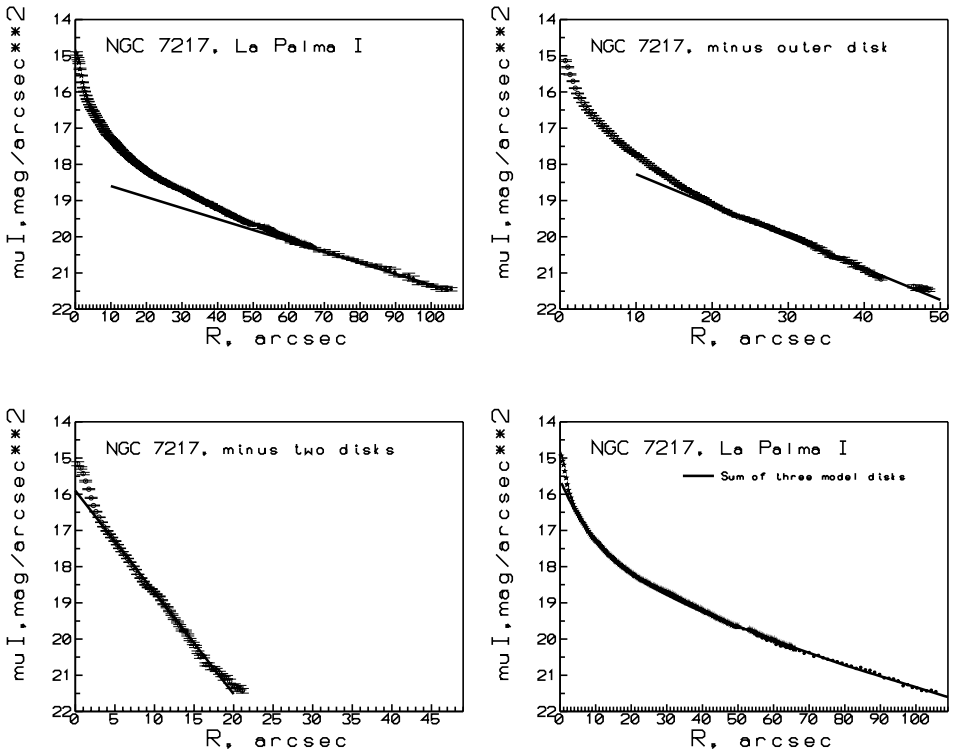

Fig. 10. Azimuthally averaged profiles of the surface brightness of NGC 7217 in the I-band. The results of recurrent fitting by exponential laws are presented at every step for the residual brightnesses, and the final result of fitting the initial total profile by 3 exponential disks with parameters given in Table 3 is shown in the right bottom panel.

Table 3. Exponential parameters of the NGC 7217 image fits

Disk	Radius range of fitting	PA_0	i	μ_0, I-mag/□″	r_0, ″	r_0, kpc
Outer	60″–110″	90°	35°	18.3	35.8	2.9
Intermediate	20″–50″	60°	23°	17.4	12.5	1.0
Inner	5″–20″	82°	28°	15.9	3.9	0.3

ness profile of NGC 7217 (Zasov & Sil'chenko 1997) revealed the existence of two equally good decomposition variants: a de Vaucouleurs' bulge plus an exponential disk, with the bulge dominating over the full radius range, and a King's bulge plus an exponential disk, with the bulge being fainter than the disk in the radius range of 20″–180″. The scalelengths of the fitted disks are very similar, 42″ and 35″, respectively, but their central brightness is of course very different. Moreover, even if one considers the central part of the brightness profile only, where the bulge predominance is beyond doubt, the effective radius of the de Vaucouleurs' law diminishes when approaching the center. Obviously, the surface brightness profile of NGC 7217 is too complex to be decomposed in unique way.

Since up to now there is no convergence in the published results of the decomposition of the brightness profile of NGC 7217, we would like to propose one more variant. For this purpose we have used photometric data from the ING Archive to calculate a brightness profile in the I-band. We have converted it into the standard Cousins system by comparison with the central I measurements from Sanchez-Portal et al. (2000). We then applied a procedure of recurrent fitting, the results of which are given in Table 3 and Fig. 10. First, the parameters are determined for the outermost parts of the exponential disk, the model map of this exponential disk is subtracted from the original map, in the residual map the position angle of the major axis and the mean ellipticity are measured, an azimuthally-averaged profile of the residual brightness is calculated, and all the steps above are repeated again. Fig. 10 presents the stages of this recurrent fitting for NGC 7217. Curiously, at every step the outer parts of the profiles look exponential. The innermost of the three exponential profiles can be traced as close to the nucleus as $R = 5''$. The scalelength of the third disk is $3\farcs86$ or 0.3 kpc – about 10% from the scalelength of the first disk. Such a ratio is typical for a galaxy consisting of an exponential disk and an exponential bulge (Courteau et al. 1996), though an exponential bulge in a Sab galaxy is a quite unusual phenomenon (Andredakis et al. 1995, de Jong 1996, Moriondo et al. 1998). However this fact allows us to treat NGC 7217 as a galaxy with an exponential bulge and two exponential disks. The final residual map obtained by subtracting the three model exponential-disk images from the original I-band image of the galaxy (Fig. 11) is quite clear. One can see the stellar rings at $R = 11''$ and $R \approx 30''$, and these rings look asymmetrical: their southern halves are brighter. For a face-on disk galaxy, such as NGC 7217, it may mean either that the dust tori are thick, or that the dust (gas) disk is inclined with respect to the stellar disk harboring

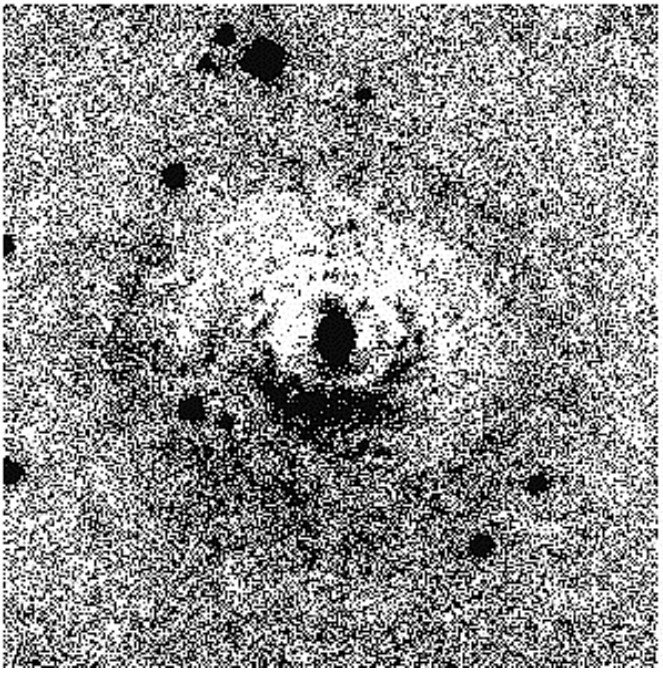

Fig. 11. The residual brightness map in the I-band after subtraction of the best-fit three-disk model. The full dimensions of the field shown are $100'' \times 100''$. North is up, east is left.

the rings, or, even more generally, that the dust and stellar rings have different inclinations because both can be inclined to the stellar disk. And finally, in the very center of the residual brightness map we see a feature which we expected to find: an oval with a major semiaxis of $4''$–$5''$ elongated in the north-south direction. This is just what we discussed at the end of the previous section: the stellar substructure corresponding to the area of maximum stellar velocity dispersion (Fig. 3, right) and of the enhanced $\langle$Fe$\rangle$ (Fig. 1, right).

6. Conclusions and discussion

We have found unique structure in the center of NGC 7217. The continuum and emission-line isophotes within $R \approx 3''$ (240 pc) are elongated approximately in the north-south direction, and the dynamical major axis of the ionized gas within $R \approx 3''$ also has $PA_0 \approx -30°$; and this coincidence shows a planar circular character of the gas rotation. However, the plane of this rotation is nearly orthogonal to the global plane of the galaxy which has a line of nodes in $PA_0 \approx 90°$. Interestingly, a similar elongation in the north-south direction is seen in the contours of the Lick $\langle$Fe$\rangle$ index distribution, whereas the magnesium-line index Mg_2 decreases quite axisymmetrically with radius. Therefore, we suggest the existence of a polar circumnuclear stellar structure, which is iron overabundant with respect to the solar abundance ratio.

Magnesium overabundant stellar systems are born when the epoch of their star formation is shorter than one billion years. Stellar systems with a solar magnesium–to–iron ratio are thought to have long and continuous star formation. To obtain iron overabundant stellar systems, chemical evolution modelists have come up with a plausible scenario: the star formation must be bursty, with pauses for a few Gyrs between the bursts. But this suggests that in the central, polarly elongated stellar structure several, at least two, discrete star formation bursts have occured. This can be related to the structure of the global disk of the galaxy, which also consists of several (three) exponential segments with different slopes. Lin & Pringle (1987) have shown that the exponential density profile of a stellar disk is a natural product of dynamical evolution when the characteristic time of the star formation is comparable to the viscous gas redistribution time, and its exponential scalelength is completely determined by the initial radius of the gaseous disk. With this idea in mind, we can propose the following scenario for the evolution of NGC 7217: in the first stage, the primordial gaseous disk was rather extended and a first stellar disk was formed with a usual scalelength, some 3 kpc. But soon a catastrophique event occured, throwing the gas suddenly toward the center by external interaction or internal instability, and the formation of the next part of the disk resulted in a smaller scalelength. The cause of this catastrophique event cannot be diagnosed in the present epoch: though the galaxy looks isolated now, it may have had small satellites some Gyrs ago which may be fully accreted after playing a role of external disturber. After a few Gyrs of quiescent star formation in the global disk of NGC 7217 a second catastrophique event occured, again gas flows into the center, and the exponential scalelength of the next, third generation component of the stellar disk (bulge?) is even smaller than that of the second. Every abrupt re-distribution of the gas along the radius had to be accompanied by a star formation burst in the center; if the temporal separation of two bursts was two to three Gyrs, this would result in iron overabundance in the central stellar concentration.

But if the central gaseous and stellar structures were formed from the gas of the global disk, why does the circumnuclear gas now rotate in the polar plane? This may be a consequence of the intrinsic dynamical evolution of the viscous subsystem. Sofue & Wakamatsu (1994) proposed that gas rotating in the plane with non-axisymmetric perturbation (e.g., a bar) passes through shocks at the edges of the bar and loses its tangential momentum first of all; it then flows into the center and there loses its radial velocity component, and finally only its vertical velocity remains unaffected. This would result in the occurence of circumnuclear gaseous polar rings (disks) in barred galaxies. Anantharamaiah & Goss (1996) reported such a ring in NGC 253, and we have found several other examples: in the Sb galaxy NGC 2841 (Sil'chenko et al. 1997b) and in the S0/a galaxy NGC 6340 (Sil'chenko 2000) the presence of a compact circumnuclear gaseous polar disks may be caused by the triaxiality of their bulges; in NGC 2841 we directly observe large-scale shocks at $R = 1 - 2$ kpc (Afanasiev & Sil'chenko 1999). In the S0 galaxy NGC 7280, which also possesses a circumnuclear gaseous polar disk, we also detected an intermediate-scale high-contrast bar with an asymmetric dust lane – a true signature of a shock (Afanasiev & Sil'chenko 2000). In NGC 7217 the clear evidence for the present or past existence of a bar is

its three rings. Buta et al. (1995) have found a low-contrast bar (more exactly, a triaxial structure) in $PA \approx 60^\circ$ by applying a Fourier analysis to a deep I-band image and showed that even such a weak perturbation may produce rings. Perhaps, this bar was stronger earlier: mass accumulation in the center had to provoke its dissolution, making it only a low-contrast feature in the present epoch. At the time when it was stronger, it could have stimulated gas inflow, accumulating it in the polar plane around the nucleus.

Acknowledgements. We thank the post-graduate student of the Special Astrophysical Observatory A. V. Moiseev for supporting the observations at the 6m telescope. The 6m telescope is operated under the financial support of Science Ministry of Russia (registration number 01-43). During the data analysis we have used the Lyon-Meudon Extragalactic Database (LEDA) supplied by the LEDA team at the CRAL-Observatoire de Lyon (France) and the NASA/IPAC Extragalactic Database (NED) which is operated by the Jet Propulsion Laboratory, California Institute of Technology, under contract with the National Aeronautics and Space Administration. This research has made use of the ING Archive. The WHT and JKT telescopes are operated on the island of La Palma by the Royal Greenwich Observatory in the Spanish Observatorio del Roque de los Muchachos of the Instituto de Astrofisica de Canarias. The research is also partly based on observations made with the NASA/ESA Hubble Space Telescope, obtained from the data archive at the Space Telescope Science Institute, which is operated by the Association of Universities for Research in Astronomy, Inc., under NASA contract NAS 5-26555. The work was supported by grant 98-02-16196 of the Russian Foundation for Basic Researches and by the Russian State Scientific-Technical Program "Astronomy. Basic Space Researches" (the "Astronomy" section).

References

Afanasiev V.L., Sil'chenko O.K., 1999, AJ 117, 1725
Afanasiev V.L., Sil'chenko O.K., 2000, AJ 119, 126
Afanasiev V.L., Vlasyuk V.V., Dodonov S.N., Sil'chenko O.K., 1990, Preprint SAO N54, Special Astrophys. Obs., Nizhnij Arkhyz
Afanasiev V.L., Dodonov S.N., Drabek S.V., Vlasyuk V.V., 1996, MPFS Manual. SAO Publ., Nizhnij Arkhyz
Anantharamaiah K.R., Goss W.M., 1996, ApJ 466, L13
Andredakis Y.C., Peletier R.F., Balcells M., 1995, MNRAS 275, 874
Athanassoula E., 1996, In: Buta R., Crocker D.A., Elmegreen B.G. (eds.) Barred Galaxies. ASP Series 91, p. 309
Baggett W.E., Baggett S.M., Anderson K.S.J., 1998, AJ 116, 1626
Block D.L., Elmegreen B.G., Wainscoat R.J., 1996, Nat 381, 674
Boroson T., 1981, ApJS 46, 177
Buta R., van Driel W., Braine J., et al., 1995, ApJ 450, 593
Cardiel N., Gorgas J., Cenarro J., Gonzalez J.J., 1998, A&AS 127, 597
Courteau S., de Jong R.S., Broeils A.H., 1996, ApJ 457, L73
de Jong R.S., 1996, A&A 313, 45
Dressler A., 1984, ApJ 286, 97
Elmegreen D.M., Chromey F.R., Bissell B.A., Corrado K., 1999, AJ 118, 2618
Emsellem E., Bacon R., Monnet G., Poulain P., 1996, A&A 312, 777
Gilmore G., Wyse R.F.G., 1991, ApJ 367, L55
Goudfrooij P., Emsellem E., 1996, A&A 306, L45
Jablonka P., Martin P., Arimoto N., 1996, AJ 112, 1415
Jore K.P., Broeils A.H., Haynes M.P., 1996, AJ 112, 438
Kent S.M., 1986, AJ 91, 1301
Laine S., Knapen J.H., Perez-Ramirez D., Doyon R., Nadeau D., 1999, MNRAS 302, L33
Lin D.N.C., Pringle J.E., 1987, ApJ 320, L87
Marconi G., Matteucci F., Tosi M., 1994, MNRAS 270, 35
Matteucci F., 1994, A&A 288, 57
Merrifield M.R., Kuijken K., 1994, ApJ 432, 575
Moriondo G., Giovanardi C., Hunt L.K., 1998, A&AS 130, 81
Peterson C.J., Rubin V.C., Ford W.K., Roberts M.S., 1978, ApJ 226, 770
Pogge R.W., 1989, ApJS 71, 433
Rubin V.C., Burstein D., Ford W.K., Thonnard N., 1985, ApJ 289, 81
Ryder S.D., Zasov A.V., McIntyre V.J., Walsh W., Sil'chenko O.K., 1998, MNRAS 293, 411
Sanchez-Portal M., Diaz A.I., Terlevich R., et al., 2000, MNRAS 312, 2
Sil'chenko O.K., 1993, Pis'ma v Astron. Zh. 19, 701
Sil'chenko O.K., 1999, Pis'ma v Astron. Zh. 25, 176
Sil'chenko O.K., 2000, AJ 120, 741
Sil'chenko O.K., Afanasiev V.L., Vlasyuk V.V., 1992, AZh 69, 1121
Sil'chenko O.K., Burenkov A.N., Vlasyuk V.V., 1997a, New Astronomy 3, 15
Sil'chenko O.K., Vlasyuk V.V., Burenkov A.N., 1997b, A&A 326, 941
Sofue Y., Wakamatsu K.-I., 1994, AJ 107, 1018
Tantalo R., Chiosi C., Bressan A., 1998, A&A 333, 419
Thornley M.D., Mundy L.G., 1997, ApJ 484, 202
Trager S.C., Worthey G., Faber S.M., Burstein D., Gonzalez J.J., 1998, ApJS 116, 1
Vlasyuk V.V., 1993, Astrofiz. issled. (Izv. SAO RAS) 36, 107
Whitemore B.C., Schechter P.L., Kirshner R.P., 1979, ApJ 234, 68
Worthey G., 1994, ApJS 95, 107
Worthey G., Faber S.M., Gonzalez J.J., 1992, ApJ 398, 69
Worthey G., Faber S.M., Gonzalez J.J., Burstein D., 1994, ApJS 94, 687
Zasov A.V., Sil'chenko O.K., 1997, AZh 74, 824